

The oxidation of WC-Co knives in wood extract

MAREK BARLAK¹, JACEK WILKOWSKI², KRZYSZTOF OSTROWSKI², ZBIGNIEW WERNER¹,
JERZY ZAGÓRSKI¹

¹Plasma/Ion Beam Technology Division, Material Physics Department, National Centre for Nuclear Research Świerk, 7 Andrzeja Sołtana St., 05-400 Otwock, Poland;

²Department of Mechanical Processing of Wood, Institute of Wood Sciences and Furniture, Warsaw University of Life Sciences, 159 Nowoursynowska St., 02-776 Warsaw, Poland;

Abstract: *The oxidation of WC-Co knives in wood extract.* The virgin WC-Co knives for wood machining and those implanted with Mg, Cr, Zn and Ni were corroded in pH 4 wood extract. A change of oxygen content throughout the experiment was determined using EDS method. The obtained results suggest a passivation of the corroded WC-Co material implanted with selected elements.

Keywords: WC-Co indexable knives, ion implantation, wood extract, oxidation, EDS method

INTRODUCTION

The cemented tungsten carbides - a combination the hard and brittle carbides and a relatively soft and ductile metallic binder, gives an exceptional combination of attractive properties such as strength, hardness, fracture toughness, refractoriness, stiffness, resistance to compressive deformation and wear resistance at room temperature as well as at higher temperatures up to 400°C (Milman et al. 1997, Sheikh-Ahmad and Bailey 1999, Pirso et al. 2004, Bonny et al. 2010, Choi et al. 2010, Olovsjö 2013).

WC-Co tools used for wood machining are exposed to a series of interactions, including corrosion. J.H. Potgieter et al. show in Ref. (Potgieter et al. 2014), that cemented carbide with Co binder practically does not passivate. Only, WC-Co pseudo passivation behaviour was observed. This material is susceptible to corrosion in each environment. The cobalt binder phase corrodes mainly in the acid and neutral media, where WC particles are corrosion resistant. In the contrary, WC phase shows active dissolution at alkaline pH, where metallic binder passivates (Potgieter et al. 2014, Tarragó et al. 2014)

Wood is a corrosive material by its nature. There are three ways of corrosion by wood (Corrosion of metals by wood, Umney 1992):

1. non-contact corrosion caused by vapours of the evaporating substances (e.g. acetic acid) in ill-ventilated rooms or wooden containers,
2. contact corrosion by wood acid like tannic acid, citric acid, acetic acid and formic acid and/or wood treatment chemicals (land-based-structures),
3. contact corrosion, where macro-galvanic mechanism predominate (immerse structures).

Wood can act as a source of corrosion for the museum exhibits or the stored tools (wooden boxes), working tools, both metal tools and ceramic-metal tools (contact with wood substances), etc. For example, it has been shown that the chemical attack by the wood acids accelerates the degradation process of WC-Co. The oxidized (corroded) cobalt binder is preferentially removed from this material thus subjecting the exposed carbide grains to increased mechanical wear (Sacks 2002).

During our investigation, the following question arose: How will the introduction of an additional element to WC-Co material change the oxidation of knives in wood extract?

The introduction of an additional element can be an electrochemical method for corrosion protection. Simple and commonly known cathodic protection is used to control the corrosion of metals by making them cathodes. A additional, more easily corrosive, sacrificial metal connected to the protected material acts as the anode and corrodes instead of the protected material. The additional layer on the protected material can be a protector for it. The standard electrode potential of the protecting material must be lower than that of the protected material.

Cobalt has two main oxidation states, i.e. Co^{2+} (stable oxidation state, where standard electrode potential is -0.277 V for Co/Co^{2+} electrode in electrochemical series) and Co^{3+} (rare oxidation state with $+0.418\text{ V}$ for Co/Co^{3+}). Magnesium, chromium, zinc and nickel was selected for the modification of WC-Co knives. The values of the potential of selected elements are: -2.37 V for magnesium (Mg/Mg^{2+}), -0.913 V and -0.74 V for chromium (Cr/Cr^{2+} and Cr/Cr^{3+} , respectively), -0.762 V for zinc (Zn/Zn^{2+}) and -0.25 V for nickel (Ni/Ni^{2+}) (Sacks 2002, Szereg napięciowy metali). The potential of the first three is lower than the potential of cobalt. All listed above elements are classical protecting materials, used in technique, industry and life. For example, magnesium is used for protection of the aerospace grade aluminium alloys (Pathak et al. 2012). Chromium is a commonly known alloying element, which markedly improves the corrosion resistance of e.g. steels in oxidizing media (Pawar and Utpat 2016). Cathodic protection is the principle underlying galvanized steel elements, like plates, nails or miscellaneous construction parts, which is steel protected by a thin layer of zinc (Corrosion). Nickel is used e.g. also for steel protection (Baldwin et al. 1995).

In the present work we report results of the ion implantation of all selected elements for the oxidation of WC-Co knives in wood extract.

A part of the presented results is extracted from the Engineering Dissertation of K. Ostrowski - a co-author of this paper.

METHODS AND MATERIALS

The commercially available, WC-Co indexable knives produced by Ceratizit (KCR08) with dimensions $29.5 \times 12 \times 1.5\text{ mm}^3$ and presented in Fig. 1, were used in the investigations.

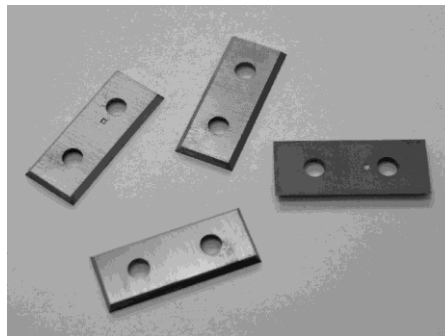


Figure 1. WC-Co indexable knives

Before processing, the knives were washed in high purity acetone under ultrasonic agitation. Next, the knives were implanted with magnesium, chromium, zinc and nickel, using MEVVA type implanter, with non mass-separated ion beam, described in detail elsewhere (Bugaev et al. 1995). Two charge state ions are used for implantation of Mg and Zn, three for Ni and four for Cr beam. All details are shown in Table 1.

Table 1. The percentage charge state distribution and average charge state of the ions implanted to WC-Co knives (Krivonosienko et al. 2001)

Cathode material	Percentage charge state distribution (%)				Average charge state
	1+	2+	3+	4+	
	Ion energy for acceleration voltage of 50 kV (keV)				
	50	100	150	200	
Mg	51	49	-	-	1.5
Cr	14	70	15	1	2.0
Zn	80	20	-	-	1.6
Ni	43	50	7	-	1.2

The implanted fluence was at a level of $3e17 \text{ cm}^{-2}$ and the acceleration voltage was 50 kV for all cases. 5N purity argon was used as the inert working gas. Vacuum in the implanter working chamber was at a level from 2 to $5e-4$ Pa. To avoid overheating effects, the samples were clamped onto a water-cooled stainless steel plate and the ion current densities were kept below 10 mA/cm^2 , so the substrate temperature did not exceed 200°C .

The ion implantation processes were preceded by Monte Carlo simulation of the main parameters of the depth profile of the implanted elements, using freeware type code The Stopping and Range of Ions in Matter - SRIM-2013.00 (Interactions of ions with matter). The simulation was performed for 100 000 implanted ions. The modelled substrate material W-C-Co (modelling codes treat the sample as a set of atoms that do not form chemical compounds) of a composition: 90.86% of tungsten, 5.94% of carbon and 3.2% of cobalt in weight percentages i.e. 47.4% of tungsten, 47.4% of carbon and 5.2% of cobalt in atomic percentages. The substrate material density, adopted for the simulation was 15.2 g/cm^3 . This value was declared by the knives supplier.

In all cases, the simulations were performed for the total implanted fluence of $3e17 \text{ cm}^{-2}$, including percentage charge state distribution data from Table 1. The modelling did not take into account the phenomenon of the substrate sputtering by the implanted ions. The theoretical values of the sputtering yield, were calculated with the use the freeware type quick ion implantation calculator SUSPRE, from the energy deposited in the surface region of the material using the Sigmund formula (SUSPRE).

Parallel with the ion implantation processes, a solution simulating a corrosive environment was prepared. The demineralized water and oak chips with humidity of 6-8% were used in the mass ratio of 9:1. The mixture of these was closed in the hermetic vessel for 1 week in the normal conditions, for the extraction of the organic compounds from wood (among other tannic acid). After this time, the oak chips were separated from the prepared solution. The pH value of this solution was 4 ± 0.1 and it was a constant throughout the experiment. The pH value was measured using CP-551 microcomputer pH meter by Elmetron company.

The virgin (non-modified) and the modified knives were corroded in the normal conditions, using the special corrosion stand, presented schematically in Fig. 2. This stand was supposed to imitate the work of the tool e.g. during cutting wood. The samples were attached into the rotating reel and periodically immersed in the corrosive solution. The rotation speed was 50 rpm.

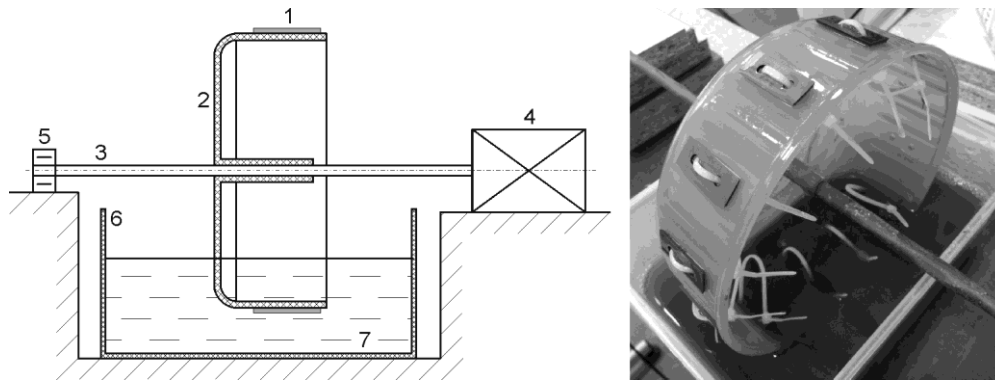


Figure 2. The scheme of the corrosion stand: 1- sample, 2 - reel, 3 - shaft, 4 - electric motor, 5 - ball bearing, 6 - vessel, 7 - solution (left) and the view of the main part of the system (right)

The virgin and the modified samples were examined before corrosion process (0 days) and after 11, 22 and 33 days of the corrosion, with the naked eyes and with the use of Zeiss EVO® MA10 scanning electron microscopy (SEM) with EDX Bruker XFlash Detector 5010 energy dispersive spectroscopy system (EDS) + dedicated Quantax 200, Esprit 1.9 code (QUANTAX EDS). A fast (300 s/measurement) less precise standardless ZAF method was used, which accounts for correction coefficients for atomic number Z, absorption A and fluorescence F (Mikroanaliza rentgenowska).

The naked eye observations allowed to estimate the colour change of the sample surface.

SEM observations of the microstructure were intended to indicate a typical places on the knives surfaces for EDS measurements. Both investigations were provided mainly for the magnification of $\times 1000$ and for the accelerating voltage of 20 kV, using SE (secondary electrons) and EDX detector, respectively. The area of the analysis for the magnification of $\times 1000$ was about $269 \times 192 \mu\text{m}^2$. The projected range of 20 keV electrons in WC was calculated by Quantax code. Totally, 6 measurement points at 2 samples from each group were taken to the calculation of average oxygen content.

Because, EDS method is relatively a little popular in this application, a few words of the description is presented in the next paragraphs.

Energy Dispersive X-ray Spectroscopy is a chemical analytical technique used in conjunction with scanning electron microscopy, for the qualitative and quantitative elemental analysis or chemical characterization of samples (Energy Dispersive X-Ray Spectroscopy). Few words about this method is presented below, because, this method is relatively new in wood industry. Fig. 3 presents the idea of the EDS method.

A high energy electron beam is focused on the investigated sample to stimulate the emission of the characteristic X-rays. In the first step, an electron from the beam (1) excites for example an electron from K electron shell with the energy E_0 (2). In the second step, electron from L shell with the energy E_1 (3), or from M shell with the energy E_2 (3'), or from N shell with the energy E_3 (3''), etc. fills the created electron hole. In the third step, the characteristic X-ray with ΔE energy $E_1 - E_0$, or $E_2 - E_0$, or $E_3 - E_0$, respectively, is generated and detected by EDS detector.

The characteristic energy emitted during electron jump from L to K shell is marked as $K\alpha$, from M to K shell - as $K\beta$, from N to K shell - as $K\gamma$, from M to L shell - as $L\alpha$, from N to L shell - as $L\beta$, etc.

The values of the characteristic energy for the substrate elements, implanted elements and oxygen are presented in Table 2. The bold values were used to the calculation of the quantity of the each element. Oxygen was determined via net-count ratios.

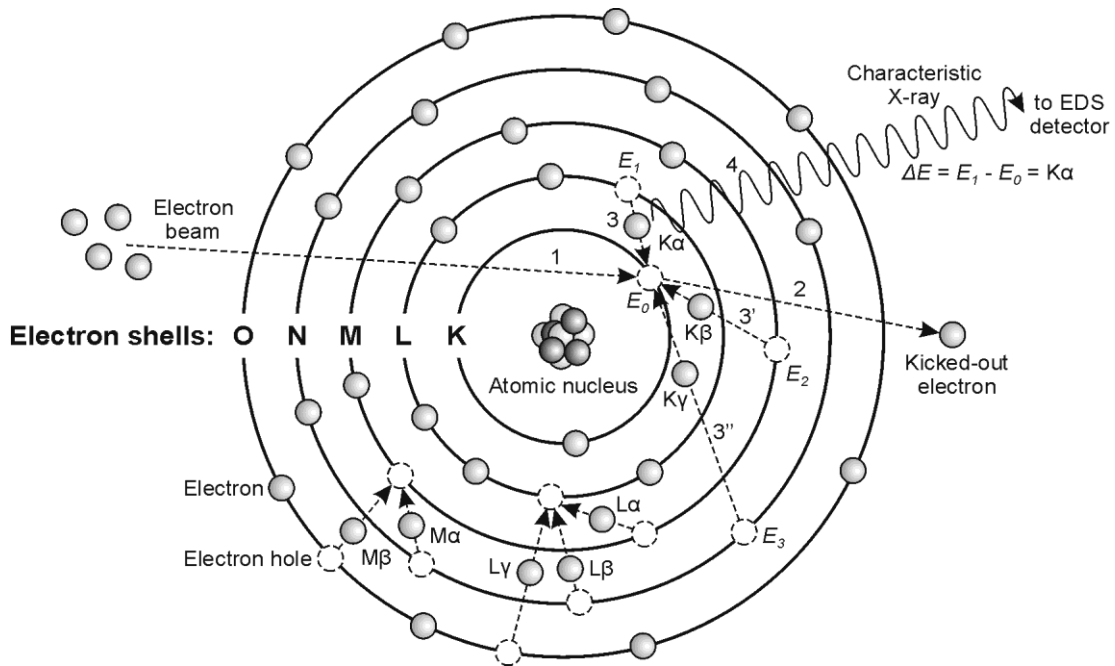


Figure 3. The idea of EDS method

Table 2. The values (in keV) of X-ray energies for the substrate elements, implanted elements and oxygen (Periodic table of elements and X-ray energies)

Atomic number	Element	K α	K β	L α	L β	M α	M β
6	Carbon C	0.277	-	-	-	-	-
8	Oxygen O	0.525	-	-	-	-	-
12	Magnesium Mg	1.254	1.302	-	-	-	-
24	Chromium Cr	5.415	5.947	0.572	0.582	-	-
27	Cobalt Co	6.931	7.649	0.775	0.790	-	-
28	Nickel Ni	7.480	8.267	0.849	0.866	-	-
30	Zinc Zn	8.637	9.570	1.012	1.035	-	-
74	Tungsten W	59.318	67.244	8.398	9.672	1.775	1.838

RESULTS AND DISCUSSION

Fig. 4 and Table 3 present the results of the computer simulations of the main parameters and the depth profiles of ions implanted without the mass separation to W-C-Co material.

The maximum value of the peak volume dopant concentration is observed for zinc ions, and the minimum - for magnesium. The difference is more than three fold.

The maximum values of the projected range and the range straggling are for magnesium ions and the minimum - for zinc. In this case, the difference is about three fold.

The values of the sputtering yield were: 1.1, 2.67, 3.61 and 3.23 atoms/ion for the ion implantation of Mg, Cr, Zn and Ni, respectively.

Colour of the corroded samples changed during the investigations (not shown here). Usually, the change was from silvery, through silvery-yellow to yellow or yellow-blue. This indicates the formation of oxide layers on the sample surfaces.

Fig. 5 shows EDS spectra for WC-Co implanted with Cr and oxidized for 0, 11, 22 and 33 days. The characteristic peaks for W (L α , L β , M α), C (K α), Co (K α), Cr (K α) and O (K α) are visible. For a better visibility, the oxygen peaks were enlarged and presented in the upper right-hand corner of the picture.

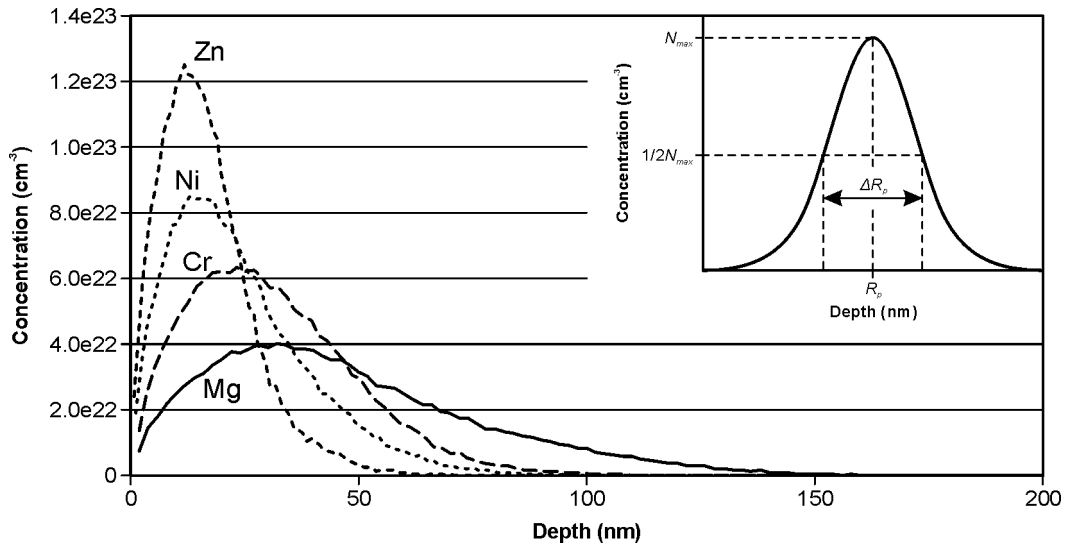


Figure 4. The depth profiles of ions implanted to W-C-Co material

Table 3. Detailed parameters of Mg, Cr, Zn and Ni ion implantation

Ions	Peak volume dopant concentration N_{max} (cm ⁻³)	Projected range R_p (nm)	Range straggling ΔR_p (nm)
Mg ⁺ + Mg ²⁺	4.02e22	46.7	29.4
Cr ⁺ + Cr ²⁺ + Cr ³⁺ + Cr ⁴⁺	6.34e22	30.3	18.0
Zn ⁺ + Zn ²⁺	1.25e23	16.3	10.1
Ni ⁺ + Ni ²⁺ + Ni ³⁺	8.49e22	23.3	15.3

The depth of all modelled and described above profiles are smaller than the projected range of 20 keV electrons in WC material, which was determined by Quantax code as about 700 nm, so all the obtained data include the modified region.

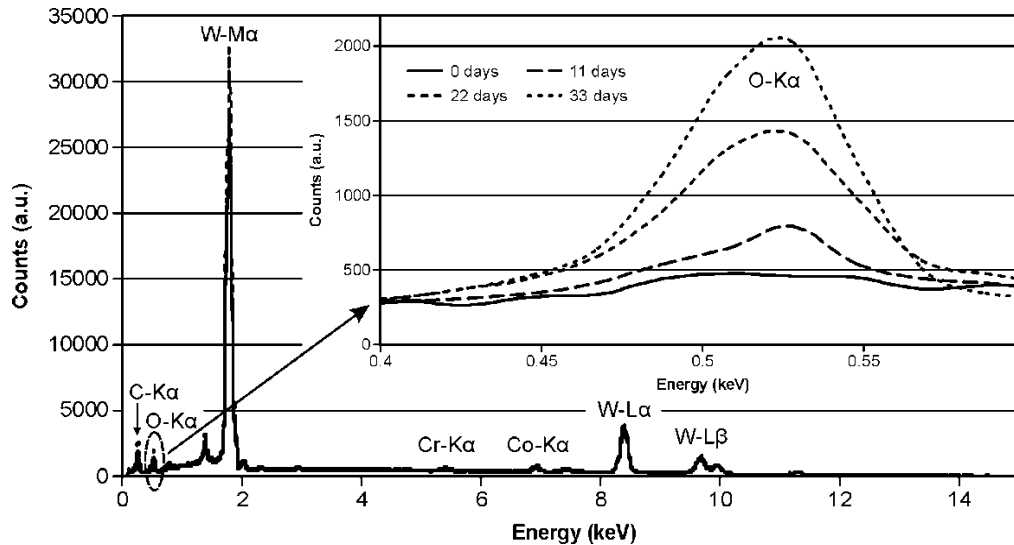


Figure 5. EDS spectra for WC-Co implanted with Cr and oxidized for 0, 11, 22 and 33 days

Fig. 6 presents oxygen content for virgin material and for all types of the modification, for 0, 11, 22 and 33 days. The standard deviation values, indicating oxygen homogeneity of the surface of the tested samples, were marked by the error bars.

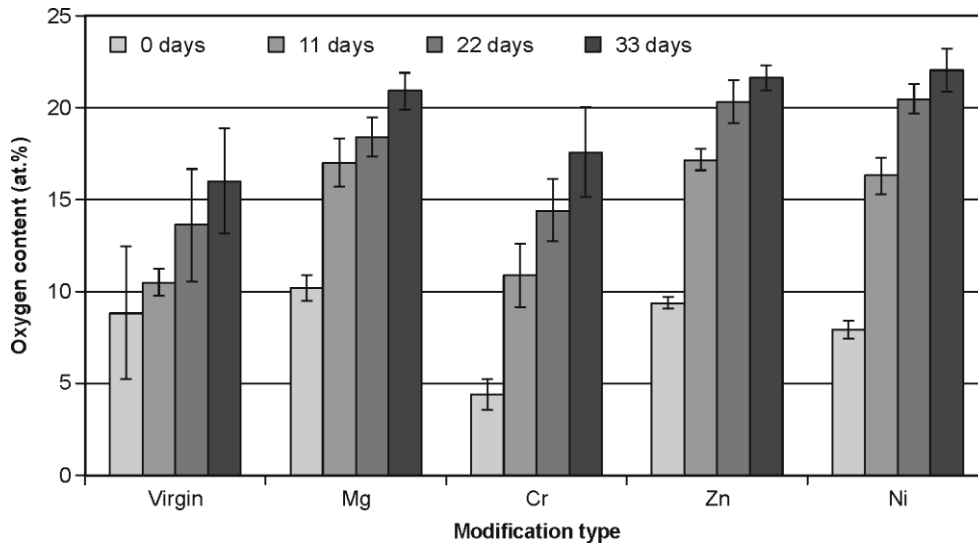


Figure 6. Oxygen content for virgin material and for all types of the modification

It is seen, that oxygen content permanently increased during the whole test for all cases. Final oxygen content was the smallest for virgin WC-Co material (16 at.%) and the largest - for WC-Co implanted with Ni (22.04 at.%). The final values of oxygen content recorded for knives implanted with Zn and Mg, i.e. 21.6 at. % and 20.91 at.%, respectively, were similar to Ni case. The discussed value for Cr modification was 17.58 at.% and it was the higher only about 10% in the comparison to the virgin material.

The virgin material was the most inhomogeneous in terms of oxygen content - the standard deviation values were the largest. Also, WC-Co material implanted with Cr showed the great oxygen heterogeneity in the comparison to other implanted cases. Much more oxygen homogeneous was WC-Co implanted with Zn, and then with Ni and with Mg.

Fig. 7 shows the nature of the changes of oxygen content more precisely. This picture presents the relative increase of oxygen content relative to the content for 0 day case (upper part) and relative content for previous point, i.e. 11 days to 0 days case, 22 days to 11 days case and 33 days to 22 days case (lower part).

The upper graphs are almost linear. The linear trend lines for these (not shown here), determined by Microsoft Excel 2010 spreadsheet, can be described by equations:

$$\begin{aligned}
 y &= 2.835x - 11.027 && \text{for Co (virgin material)} && (1) \\
 y &= 1.742x + 45.746 && \text{for Mg} && (2) \\
 y &= 6.888x + 72.266 && \text{for Cr} && (3) \\
 y &= 2.148x + 62.779 && \text{for Zn} && (4) \\
 y &= 3.279x + 74.43 && \text{for Ni} && (5)
 \end{aligned}$$

The values of the coefficient of determination R^2 are: 0.994, 0.976, 0.999, 0.946 and 0.936 for Co (virgin), Mg, Cr, Zn and Ni, respectively.

The value of the factor “a” from the equation $y = ax + b$ was used in the analysis of the nature of the change of the amount of oxygen in the corroded samples. It was assumed that the higher the value of the factor “a”, the greater the increase in the oxygen content in samples.

It is seen, that for the largest increase in the amount of oxygen is for WC-Co material implanted with Cr, and the smallest - for Mg implantation. The change for virgin material (oxidation of Co) has a slightly different character (the negative factor “b” in the discussed equation).

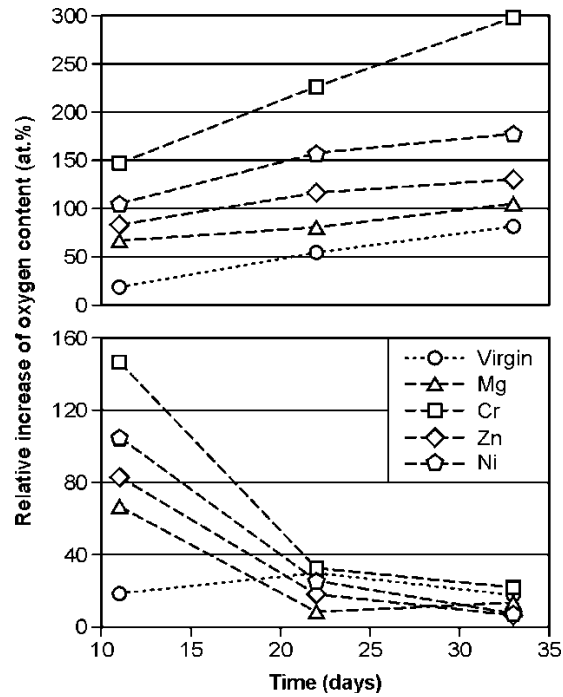


Figure 7. The relative increase of oxygen content relative to the content for 0 day case (upper part) and relative content for previous point (lower part)

For the lower part of Fig. 7, the equation of the second-degree polynomial is more appropriate to describe the change nature:

$$y = -0.096x^2 + 4.155x - 15.348 \quad \text{for Co (virgin material)} \quad (6)$$

$$y = 0.262x^2 - 13.952x + 188.4 \quad \text{for Mg} \quad (7)$$

$$y = 0.428x^2 - 24.515x + 364.46 \quad \text{for Cr} \quad (8)$$

$$y = 0.219x^2 - 13.138x + 201.13 \quad \text{for Zn} \quad (9)$$

$$y = 0.255x^2 - 15.646x + 246.33 \quad \text{for Ni} \quad (10)$$

The value of the factor “a” from the equation $y = ax^2 + bx + c$ was used also here to the analysis of the nature of the change of the amount of oxygen, similarly to the previous case.

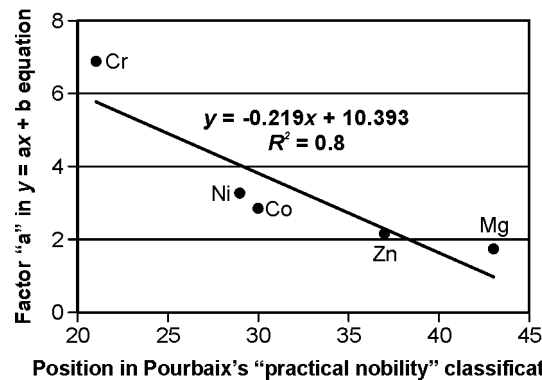
In this case, also the largest increase in the amount of oxygen is for Cr implantation, but the smallest - for Zn. Also, the change for virgin material (oxidation of Co) is different in the comparison to others (the negative factor “a” in the equation).

M. Pourbaix in Ref. (Pourbaix 1978) classified 43 elements in the order of “thermodynamic nobility”, which includes only the immunity and “practical nobility”, which includes the immunity and the passivation. The order (from more noble to less noble) of the elements implanted to WC-Co for both classifications is presented in Table 4, in two first columns. The position of each elements in the selected classification is shown in the round brackets. Additionally, the data for Co were shown.

The order of the implanted elements, deduced from “a” factor from the equations (2)-(5) and (7)-(10) is presented in two next columns. It is easy to see that the data in columns 2 and 3 are identical. This correlation was presented graphically in Fig. 8, where the points are arranged near a straight line with the equation $y = -0.219x + 10.393$ and the coefficient of determination $R^2 = 0,8$ (by Microsoft Excel 2010 spreadsheet). It can suggest the phenomenon of the passivation of WC-Co implanted with selected ions.

Table 4. The juxtaposition of the part of Pourbaix's classifications with the obtained results

Pourbaix's classifications		Results presented in Fig. 7	
Thermodynamic nobility	Practical nobility	Upper part	Lower part
Ni (21)	Cr (21)	Cr	Cr
Co (22)	Ni (29)	Ni	Mg
Zn (32)	Co (30)	Co	Ni
Cr (35)	Zn (37)	Zn	Zn
Mg (43)	Mg (41)	Mg	Co

**Figure 8.** The correlation of the position of Cr, Ni, Co, Zn and Mg in Pourbaix's "practical nobility" classification with the data for these elements deduced from equations (1)-(5)

CONCLUSIONS

Oxidation of WC-Co knives in wood extract, like each chemical process, is a very complex issue, which depends on many factors. Based on presented work, we can only conclude that:

1. the modelled/calculated values of the peak volume concentration, the projected range, the range straggling and the sputtering yield for all implanted elements do not correlate with the amount of oxygen in the samples,
2. a comparison the obtained results and the Pourbaix's classifications suggests that the passivation is the most likely phenomenon in the implanted and oxidized material,
3. different features of the data obtained for non-passivating cobalt may indicate material corrosion.

At this moment, the form of oxygen (oxides), the new chemical phases in the implanted and oxidized WC-Co and their relationship with the oxidation processes remain unknown. It will be the subject of our next investigations.

Acknowledgments: The authors wish to thank Dr. P. Kołodziejczak for the idea of the corrosion stand.

REFERENCES

1. BALDWIN K.R., SMITH C.J.E., ROBINSON M.J., 1995: Cathodic protection of steel by electrodeposited zinc-nickel alloy coatings, *Corrosion*, 51; 932-940. DOI: 10.5006/1.3293569
2. BONNY K., DE BAETS P., PEREZ Y., VLEUGELS J., LAUWERS B., 2010: Friction and wear characteristics of WC-Co cemented carbides in dry reciprocating sliding contact, *Wear*, 268; 1504-1517. DOI: 10.1016/j.wear.2010.02.029
3. BUGAEV S.P., NIKOLAEV A.G., OKS E.M., SCHANIN P.M., YUSHKOV G.YU., 1994: The "TITAN" ion source, *Review of Scientific Instruments*, 65; 3119-3125. DOI: 10.1063/1.1144765

4. CHOI S.-H., KANG S.-D., KWON Y.S., LIM S.G., CHO K.K., AHN I.-S., 2010: The effect of sintering conditions on the properties of WC-10wt%Co PIM compacts, *Research on Chemical Intermediates*, 36; 743-748. DOI: 10.1007/s11164-010-0176-8
5. Corrosion [https://chem.libretexts.org/Bookshelves/General_Chemistry/Map%3A_Chemistry_\(Zumdahl_and_Decoste\)/11%3A_Electrochemistry/11.6%3A_Corrosion](https://chem.libretexts.org/Bookshelves/General_Chemistry/Map%3A_Chemistry_(Zumdahl_and_Decoste)/11%3A_Electrochemistry/11.6%3A_Corrosion)
6. Corrosion of metals by wood, http://resource.npl.co.uk/docs/science_technology/materials/life_management_of_materials/publications/online_guides/pdf/corrosion_of_metals_by_wood.pdf
7. Energy Dispersive X-Ray Spectroscopy (EDS), <https://www.mee-inc.com/hamm/energy-dispersive-x-ray-spectroscopyeds/>
8. Interactions of ions with matter, <http://www.srim.org/>
9. KRIVONOSIENKO A.W., NIKOLAEV A.G., LI S., 2001: Технические описание и инструкция по эксплуатации ионного источника “Титан-3” (Technical descriptions and operating instructions of the ion source “Titan-3”), Российская Академия Наук - Институт Сильноточной Электроники, Томск, in Russian.
10. MIKROANALIZA RENTGENOWSKA. http://www.imim.pl/files/Wykladyprof_MF/Wyklad%20IV%20doktoranci.pdf
11. MILMAN. Y.V., CHUGUNOVA S., GONCHARUCK V., LUYCKX S., NORTHROP I.T., 1997: Low and high temperature hardness of WC-6 wt%Co alloys, *International Journal of Refractory Metals and Hard Materials*, 15; 97-101. DOI: 10.1016/S0263-4368(97)81231-0
12. OLOVSJÖ S., JOHANSON R., FALSAFI F., BEXELL U., OLSSON M., 2013: Surface failure and wear of cemented carbide rock drill buttons - The importance of sample preparation and optimized microscopy settings, *Wear*, 302; 1546-1554. DOI: 10.1016/j.wear.2013.01.078
13. PATHAK S.S., MENDON S.K., BLANTON M.D., RAWLINS J.W., 2012: Magnesium-based sacrificial anode cathodic protection coatings (Mg-rich primers) for aluminum alloys, *Metals* 2; 353-376. DOI: 10.3390/met2030353
14. PAWAR P.B., UTPAT A.A., 2016: Effect of chromium on mechanical properties of A487 stainless steel alloy, *International Journal of Advance Research in Science and Engineering*, 5; 112-118. DOI: 10.13140/RG.2.2.13846.04163
15. Periodic table of elements and X-ray energies, https://www.bruker.com/fileadmin/user_upload/8-PDF-Docs/X-rayDiffraction_ElementalAnalysis/HH-XRF/Misc/Periodic_Table_and_X-ray_Energies.pdf
16. PIRSO J., LETUNOVITŠ S., VILJUS M., 2004: Friction and wear behaviour of cemented carbides, *Wear*, 257; 257-265. DOI: 10.1016/j.wear.2003.12.014
17. POTGIETER J.H., OLUBAMBI P., POTGIETER-VERMAAK S.S., 2014: The corrosion behaviour of WC-Co-Ru alloys in aggressive chloride media, *International Journal of Electrochemistry*, 2014; 594871. DOI: 10.1155/2014/594871
18. POURBAIX M., 1978: Wykłady z korozji elektrochemicznej, Państwowe Wydawnictwo Naukowe, Warsaw, in Polish.
19. QUANTAX EDS - User Manual, <http://emc.missouri.edu/wp-content/uploads/2016/01/Bruker-Quantax-EDS-User-Manual.pdf>
20. SACKS N., 2002: The wear and corrosive-wear response of tungsten carbide-cobalt hardmetals under woodcutting and three body abrasion conditions, Doktor-Ingenieur degree, University of Erlangen-Nürnberg, Erlangen.
21. SHEIKH-AHMAD J.Y., BAILEY J.A., 1999: High-temperature wear of cemented tungsten carbide tools while machining particleboard and fibreboard, *Journal of Wood Science*, 45; 445-455. DOI: 10.1007/BF00538952

22. SUSPRE, <https://www.surrey.ac.uk/ion-beam-centre/research-areas/interactions-energetic-particles>
23. Szereg napięciowy metali Ogniwa galwaniczne, http://www.chemia.odlew.agh.edu.pl/dydaktyka/Dokumenty/ChO_WO/Niestacjonarne/szereg_zao.pdf, in Polish.
24. TARRAGÓ J.M., FARGAS G., JIMENEZ-PIQUÉ E., FELIP A., ISERN L., COUREAUX D., ROA J.J., AL-DAWERY I., FAIR J., LLANES L., 2014: Corrosion damage in WC-Co cemented carbides: Residual strength assessment and 3D FIB-FESEM tomography characterization, *Powder Metallurgy*, 57; 324-330. DOI: 10.1179/1743290114Y.0000000115
25. UMNEY N., 1992: Corrosion of metals associated with wood, *Conservation Journal* 04, <http://www.vam.ac.uk/content/journals/conservation-journal/issue-04/corrosion-of-metals-associated-with-wood/>

Streszczenie: *Utlenianie noży WC-Co w ekstrakcie drzewnym.* Wyjściowe noże WC-Co do obróbki drewna oraz noże implantowane jonami Mg, Cr, Zn i Ni zostały poddane korozji w ekstrakcie drzewnym o wartości pH 4. Zmianę zawartości tlenu w trakcie eksperymentu oznaczono metodą EDS. Uzyskane wyniki sugerują wystąpienie zjawiska pasywacji utlenianego materiału WC-Co implantowanego wybranymi pierwiastkami.

Corresponding author:

Marek Barlak
7 Andrzeja Sołtana St.
05-400 Otwock, Poland
email: marek.barlak@ncbj.gov.pl
phone: +48 22 273 16 44